




Physiological clearance of tau in the periphery and its therapeutic potential for tauopathies

Jun Wang¹ · Wang-Sheng Jin¹ · Xian-Le Bu¹ · Fan Zeng¹ · Zhi-Lin Huang³ · Wei-Wei Li¹ · Lin-Lin Shen¹ · Zhen-Qian Zhuang¹ · Yuqiang Fang⁴ · Bin-Lu Sun¹ · Jie Zhu¹ · Xiu-Qing Yao¹ · Gui-Hua Zeng¹ · Zhi-Fang Dong³ · Jin-Tai Yu⁵ · Zhian Hu⁶ · Weihong Song⁷ · Hua-Dong Zhou¹ · Jian-Xin Jiang² · Yu-Hui Liu¹ · Yan-Jiang Wang^{1,2,8} 

Received: 14 February 2018 / Revised: 18 July 2018 / Accepted: 18 July 2018 / Published online: 3 August 2018
© Springer-Verlag GmbH Germany, part of Springer Nature 2018

Abstract

Accumulation of pathological tau is the hallmark of Alzheimer's disease and other tauopathies and is closely correlated with cognitive decline. Clearance of pathological tau from the brain is a major therapeutic strategy for tauopathies. The physiological capacity of the periphery to clear brain-derived tau and its therapeutic potential remain largely unknown. Here, we found that cisterna magna injected ¹³¹I-labelled synthetic tau dynamically effluxed from the brain and was mainly cleared from the kidney, blood, and liver in mice; we also found that plasma tau levels in inferior vena cava were lower than those in femoral artery in humans. These findings suggest that tau proteins can efflux out of the brain and be cleared in the periphery under physiological conditions. Next, we showed that lowering blood tau levels via peritoneal dialysis could reduce interstitial fluid (ISF) tau levels in the brain, and tau levels in the blood and ISF were dynamically correlated; furthermore, tau efflux from the brain was accelerated after the addition of another set of peripheral system in a parabiosis model. Finally, we established parabiosis mouse models using tau transgenic mice and their wild-type littermates and found that brain tau levels and related pathologies in parabiotic transgenic mice were significantly reduced after parabiosis, suggesting that chronic enhancement of peripheral tau clearance alleviates pathological tau accumulation and neurodegeneration in the brain. Our study provides the first evidence of physiological clearance of brain-derived pathological tau in the periphery, suggesting that enhancing peripheral tau clearance is a potential therapeutic strategy for tauopathies.

Keywords Tauopathy · Parabiosis · Peritoneal dialysis · Tau · Clearance · Periphery

Electronic supplementary material The online version of this article (<https://doi.org/10.1007/s00401-018-1891-2>) contains supplementary material, which is available to authorized users.

✉ Yu-Hui Liu
liuyuhui07-8909@163.com

✉ Yan-Jiang Wang
yanjiang_wang@tmmu.edu.cn

¹ Department of Neurology, Daping Hospital, Third Military Medical University, Chongqing, China

² State Key Laboratory of Trauma, Burn and Combined Injury, Institute of Surgery Research, Daping Hospital, Third Military Medical University, Chongqing, China

³ Ministry of Education Key Laboratory of Child Development and Disorders, Chongqing Key Laboratory of Translational Medical Research in Cognitive Development and Learning and Memory Disorders, Children's Hospital of Chongqing Medical University, Chongqing, China

⁴ Department of Cardiology, Daping Hospital, Third Military Medical University, Chongqing, China

⁵ Department of Neurology, Qingdao Municipal Hospital, School of Medicine, Qingdao University, Qingdao, China

⁶ Department of Physiology, Collaborative Innovation Center for Brain Science, Third Military Medical University, Chongqing, China

⁷ Townsend Family Laboratories, Department of Psychiatry, Brain Research Center, The University of British Columbia, Vancouver, BC V6T 1Z3, Canada

⁸ Center for Excellence in Brain Science and Intelligence Technology, Chinese Academy of Sciences, Shanghai, China

Introduction

Tauopathies are progressive neurodegenerative disorders that include, but are not limited to, Alzheimer's disease (AD), progressive supranuclear palsy (PSP), corticobasal degeneration (CBD), Pick's disease, certain forms of frontotemporal lobar degeneration (FTLD), and chronic traumatic encephalopathy [18, 29]. Tau is an abundant, highly soluble intracellular protein that binds to microtubules and promotes their stability [12]. However, in tauopathies, tau aggregates and accumulates in hyperphosphorylated neurofibrillary tangles (NFTs) that occur in neurons and dystrophic neurites [28]. The amount of abnormally hyperphosphorylated tau, or tau pathology, is well correlated with neuronal loss, synaptic dysfunction, and cognitive decline [5, 22, 44]. Unfortunately, effective therapies for tauopathies are lacking [7].

It is suggested that intracellular pathogenic tau can be released into the intercellular space and then enter adjacent cells, where it seeds further tau aggregation and propagates the pathology [15, 16, 25, 33]. Blocking this transmission process by removal of pathogenic tau from the intercellular space represents a promising therapeutic approach for tauopathies [7]. Recent studies suggest that brain-derived pathological tau can flow into the bloodstream [35, 45]. However, the subsequent consequences of tau efflux from the brain remain largely unknown. In the present study, we found that tau could flow from the brain into the blood stream and be physiologically cleared in peripheral tissues and organs; enhancement of peripheral tau clearance is able to reduce brain pathological tau levels, suggesting that peripheral tau clearance represents a potential therapeutic strategy for tauopathies.

Materials and methods

Participants and blood sampling

The human study protocol was approved by the Ethics Committee of Daping Hospital affiliated with Third Military Medical University. This study enrolled a total of 20 patients (8 females and 12 males) who suffered from atrioventricular re-entrant tachycardia (AVRT) and underwent radiofrequency catheter ablation (RFCA) from Daping Hospital and The Third Affiliated Hospital of Chongqing Medical University (Supplemental Table 1). The average age of these patients was 52.4 years old (35–75 years). Blood was collected from the inferior vena cava (IVC) proximal to the hepatic vein and right femoral artery (FA) within a time frame of 5 min. Six millilitres of blood were collected at each site, and plasma was separated within 2 h after collection and stored at -80°C until use.

Animals

P301L tau transgenic (pR5) mice on a C57BL/6 background were provided by Professor Juergen Gotz from Queensland Brain Institute, Queensland University (Australia) and raised in Daping Hospital Animal House. The pR5 mouse model expresses the longest human tau isoform (2N4R) with the FTDP-17 mutation P301L in neurons and is characterized by hyperphosphorylation of tau at certain phosphorylation sites, which occurs in AD and other tauopathies [10, 20]. All animal experiments were approved by the Third Military Medical University Animal Welfare Committee.

Biodistribution of ^{131}I -tau after intravenous or cisterna magna injection

Radiolabelling of ^{131}I -tau was performed following the previous protocols. Synthetic human Tau441 was iodinated with Na^{131}I using the chloramine T (Ch-T) method [47]. The radiochemical purity of radioiodinated tau was $>95\%$.

For experiments assessing tau clearance in the periphery, wild-type (Wt) mice were used, and 6.7 MBq of ^{131}I -tau in 0.3 ml of normal saline was injected into the tail vein or 9.3 MBq of ^{131}I -tau was injected into the cisterna magna under anaesthesia. At 15, 30 min, 1, 4, or 8 h after injection ($n=3$ per timepoint), blood was collected via retro-orbital bleeds, and brain, skin, intestine, lung, heart, liver, spleen, kidney, bone, and muscle were collected and weighed after transcardiac perfusion. In experiments assessing effects of parabiosis on tau clearance in the brain and periphery, 9.3 MBq of ^{131}I -tau was injected into the cisterna magna of one parabiotic Wt mouse (Wt–Wt pair) and of singular Wt mice. Brain and peripheral tissues and organs were collected and weighed at different time intervals of 15 min, 1, and 4 h ($n=3$ per timepoint). The radioactivity (CPM values) of samples was measured, and the resulting counts/min values were normalized per gram of tissue. The radioactivity values are shown as counts/min/g of tissue.

Peritoneal dialysis

Six-month-old male pR5 mice were subjected to peritoneal dialysis ($n=5$). The peritoneal dialysis surgery was performed following previously described procedures [21]. An “open” permanent system was subcutaneously tunnelled from the neck to the abdomen, and one end was placed in the peritoneal cavity. For peritoneal dialysis, 2 ml of 2.5% dialysis solution (Baxter Healthcare Corporation, China. 100 ml of solution contains 2.5 g of dextrose hydrous, 538 mg of sodium chloride, 448 mg of sodium lactate, 18.3 mg of calcium chloride, and 5.1 mg of magnesium chloride) was injected into the peritoneal cavity via tubing and collected

2 h later. The recovery efficiency of peritoneal dialysis was approximately 50% (1 ml of dialysis solution).

Microdialysis

Microdialysis experiments were performed as described elsewhere [43]. A guide cannula (Eicom, Japan) was stereotactically implanted in the left hippocampus (*A/P*: – 3.1 mm, *M/L*: – 2.5 mm, *D/V*: – 1.2 mm, 12°) and cemented using binary dental cement. After a recovery period of at least 3 days, a 2-mm 1000-kDa cutoff AtmosLM microdialysis probe (Eicom, Japan) was inserted through the guide cannula. The probe was connected to a microdialysis peristaltic pump (MAB20, SciPro), which was operated in the push–pull mode. Artificial cerebral spinal fluid (ACSF) containing 4% human albumin solution was used as perfusion buffer for ISF collection. For ISF collection, a flow rate of 1 μ l/min was used. ISF samples were collected hourly in a refrigerated fraction collector.

Parabiosis

pR5 mice and their sex-matched Wt littermates were selected for parabiosis ($n=8$ per group, half female, and half male). Parabiosis surgery was performed as previously described [3, 41]. Opposing scapulae, femurs, muscle layers, and skin of the pairs of mice were fixed together. Parabiosis was performed at 3 months of age when the level of abnormal phosphorylated tau is low and NFTs have not formed in the brain; samples were collected for analysis at 6 months of age when abnormal phosphorylated tau is abundant and behavioural deficits have emerged (Supplemental Fig. 2a). Age-, sex-, and weight-matched Wt and pR5 mice without parabiosis were used in parallel as controls.

Electrophysiology

In the parabiosis experiment, a designated group of parabionts and their Wt and pR5 controls ($n=6$) were subjected to electrophysiology tests as described previously [3, 21]. Test fEPSPs were evoked at a frequency of 0.033 Hz and at a stimulus intensity that was adjusted to approximately 50% of the intensity that elicited the maximal response. After a 20-min stable baseline, long-term potential (LTP) was induced by high-frequency stimulation (HFS, 100 pulses at 100 Hz). All recordings were conducted at room temperature using a Multiclamp EPC 10 amplifier (HEKA Electronics, Lambrecht/Pfalz, Germany).

Immunohistochemistry and immunofluorescence

A series of five equally spaced tissue sections (~ 1.3-mm apart) spanning the entire brain were stained for

phosphorylated tau (rabbit anti-pS396-tau, Signalway, USA; AT100, mouse anti-PHF-tau, Invitrogen, USA) using free-floating immunohistochemistry methods [34, 46]. Briefly, selected brain sections were treated with 0.3% H₂O₂ mixed with 0.5% Triton X-100 in PBS for 30 min at room temperature, followed by blocking with 3% BSA for 30 min, and then incubated overnight with primary antibody at 4 °C. On day 2, sections were incubated with secondary antibodies conjugated with HRP for 1 h at 37 °C, followed by visualization with DAB solution for immunohistochemistry staining. Apoptosis of neuronal cells was detected by double immunofluorescence staining for NeuN (mouse anti-NeuN, Abcam, UK) and caspase-3 (rabbit anti-caspase-3, Millipore, USA). Neuronal loss and neurite degeneration were detected by double immunofluorescence staining for NeuN and microtubule-associated protein (MAP)-2 (rabbit anti-MAP-2, Millipore, USA). The fraction of positive staining as a proportion of total area was quantified with the ImageJ software.

Measurements of human plasma tau

A Simoa assay was used to measure total tau levels in human plasma collected from the inferior vena cava and femoral artery according to the manufacturer's protocol (Simoa™ Neurology 3-Plex A Advantage kit, Quanterix Simoa-HD1 Platform, Hangzhou, China) [8]. Plasma samples were analysed at a 1/4 dilution. Each batch was analysed using six standard replicate curves and by applying a four-parameter logistic fit with 1/Y² weighting.

ELISAs

For ELISAs, powdered brain samples were weighed, and protein was sequentially extracted in Tris buffer solution (TBS) and 2% sodium dodecyl sulfonate (SDS). The levels of human pT181-Tau, pT231-Tau, and total tau in the TBS and SDS fractions and microdialysis fluids, as well as the total tau concentrations in plasma, were measured using ELISA kits according to the manufacturer's instructions (Invitrogen, USA). Inflammatory factors, including TNF- α , IFN- γ , IL-1 β , and IL-6, in brain homogenates and blood were measured using corresponding ELISA kits (R&D systems, USA).

Western blotting

For Western blotting analysis, brain powder was suspended in RIPA buffer, and proteins were extracted. Identical amounts of RIPA-extracted protein were separated by SDS-PAGE (4–10% acrylamide) and transferred to nitrocellulose membranes. The blots were probed with antibodies against the following targets: pT181, pT231, pS199, pS404 (Signalway, USA), tau5 (Abcam, UK), glycogen synthase kinase

3 beta (GSK3 β ; Abcam, UK), pS9-GSK3 β (Abcam, UK), synaptosomal-associated protein 25 (SNAP-25, Millipore, USA), vesicle-associated membrane protein 1 (VAMP-1, Abcam, UK), postsynaptic density protein 93 (PSD-93, Abcam, UK), PSD-95 (Millipore, USA), the major synaptic vesicle protein p38 synaptophysin (SYP, Millipore, USA), doublecortin (DCX, Abcam, UK), neuron-specific enolase (NSE, Abcam, UK), and β -actin (Sigma-Aldrich). The membranes were incubated with IRDye 800CW secondary antibodies (Li-COR) and scanned using an Odyssey fluorescence scanner. The band density was normalized to β -actin for analysis.

Statistical analysis

The results are presented as the mean \pm SEM. Statistical analysis included a two-tailed Student's *t* test, a Mann–Whitney *U* test, or a paired *t* test, as applicable, to compare two groups; one-way ANOVA and Tukey's test were used to compare three groups, and two-way ANOVA was used to compare two groups at multiple timepoints. Normality and equal-variance testing were performed for all assays.

$p < 0.05$ was considered significant. All analyses were conducted with the GraphPad Prism 5.0 software.

Results

Tau efflux from the brain and its clearance in the periphery in mice and humans

To explore whether tau can efflux out of the brain into the blood and the physiological clearance of brain-derived tau in the periphery, we investigated the dynamic distribution of ^{131}I -tau in the brain and the periphery. After cisterna magna injection, high radioactivity levels were detected in whole blood 15 min after injection, while radioactivity in the brain declined sharply (Fig. 1a), suggesting that tau effluxed from the brain into the blood within minutes. The radioactivity in the periphery was primarily distributed in the blood and kidney, with a moderate presence in the liver, and declined over time in the blood and kidney (Fig. 1a), indicating that tau was cleared from these locations. Similarly, after intravenous injection, the radioactivity was mostly located in the

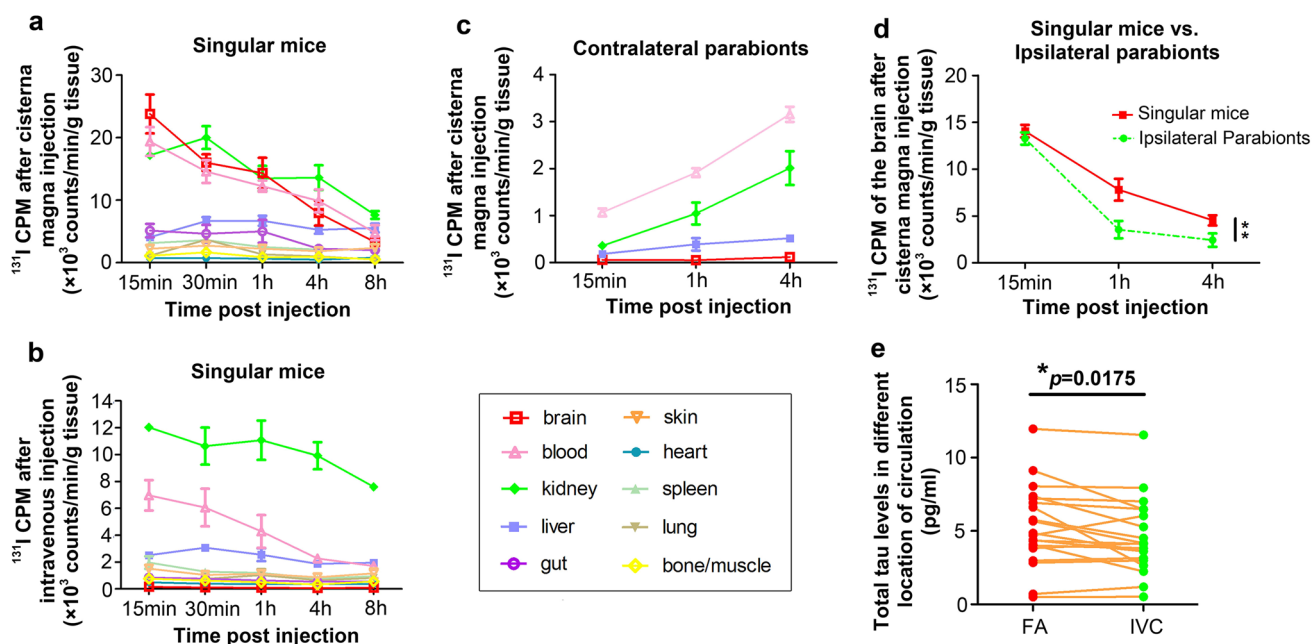


Fig. 1 Dynamic distribution of ^{131}I -labelled tau after cisterna magna or intravenous injection and tau concentrations at different locations in human systemic circulation. **a–d** Dynamic changes in radioactivity levels in the brain and periphery after injection of ^{131}I -labelled synthetic tau ($n=3$ each timepoint, two-way ANOVA). **a** Dynamic changes in radioactivity levels in the brain and periphery after injection of ^{131}I -tau in the cisterna magna. **b** Dynamic changes in radioactivity levels in the brain and periphery after intravenous injection of ^{131}I -tau. **c** Dynamic changes in radioactivity levels in the brain and periphery of parabiotic mice. Wt mice were connected as Wt–Wt parabiotic pairs. ^{131}I -tau was injected into the cisterna magna of

one parabiotic wild-type mouse (ipsilateral), and radioactivity levels were measured in the contralateral parabiotic mouse. **d** Comparison of dynamic radioactivity changes in the brain of ipsilateral parabionts or singular Wt mice after cisterna magna injection of ^{131}I -tau. For parabiotic mice, ^{131}I -tau was injected into the cisterna magna of one parabiotic wild-type mouse (ipsilateral), and radioactivity levels were measured in the ipsilateral parabiotic mouse. **e** Comparison of total tau levels between plasma samples from the femoral artery and inferior vena cava in humans ($n=20$, paired *t* test). IVC inferior vena cava, FA femoral artery. Error bar, SEM. * $p < 0.05$, ** $p < 0.01$, and *** $p < 0.001$

kidney and blood, and moderate amounts were observed in the liver (Fig. 1b), further verifying that these tissues and organs are the primary sites of tau clearance in the periphery. In addition, blood ^{131}I -tau exhibited a prolonged half-life of 4.8 h after cisterna magna injection in comparison with that of 3.4 h after intravenous injection (Supplemental Fig. 1a, b). We also injected free ^{131}I into the cisterna magna as control. At 1 h after injection, the radioactivities of free ^{131}I were extremely low, while that of ^{131}I -tau remained at a high level in the brain. Meanwhile, the radioactivities of free ^{131}I were mainly distributed in the blood, whereas those of ^{131}I -tau were primarily distributed in the blood, liver, and kidney (Supplemental Fig. 1c, d). The different patterns of dynamic biodistribution between free ^{131}I and ^{131}I -tau suggest that the radioactivities we detected in the periphery after ^{131}I -tau injection represent tau protein but not disassociated ^{131}I molecules from ^{131}I -tau.

The above results indicate that the kidney and liver are the main organs for peripheral tau clearance in animals. To investigate peripheral tau clearance by viscera in humans, we measured plasma tau levels at the femoral artery, which collects blood before flowing through viscera, and at the inferior vena cava proximal to the hepatic vein, which collects blood after it flows through the viscera. We found that total tau levels in blood from the inferior vena cava were lower than those in blood from the femoral artery (Fig. 1e, Supplemental Table 1), suggesting that tau protein in the blood was cleared when it went through the peripheral viscera under physiological conditions in humans.

Enhancing peripheral tau clearance facilitates tau efflux from the brain

To investigate whether lowering blood tau levels can lead to a reduction in tau levels in the brain, we conducted a short-term peritoneal dialysis experiment with male, 3-month-old pR5 mice and examined the dynamic interaction between the blood tau and brain ISF tau levels. ISF tau levels were reflected by the tau levels in microdialysis fluid. As shown in Fig. 2, total tau (t-tau) levels in the blood decreased immediately after peritoneal dialysis was started and reached the lowest levels 2–3 h later, followed by a slight and slow increase after peritoneal dialysis was stopped. Interestingly, the changes in tau levels in ISF paralleled those in the blood, indicating that the tau levels in ISF and blood were dynamically correlated. These findings suggest that lowering tau levels in the blood could induce a reduction in tau levels in the brain.

Next, to investigate whether enhancement of peripheral tau clearance can facilitate tau efflux from the brain, isochronic parabiosis was established between two sex-matched Wt mice at 3 months of age. After 1 month of recovery, the circulatory systems of the two parabionts were joined

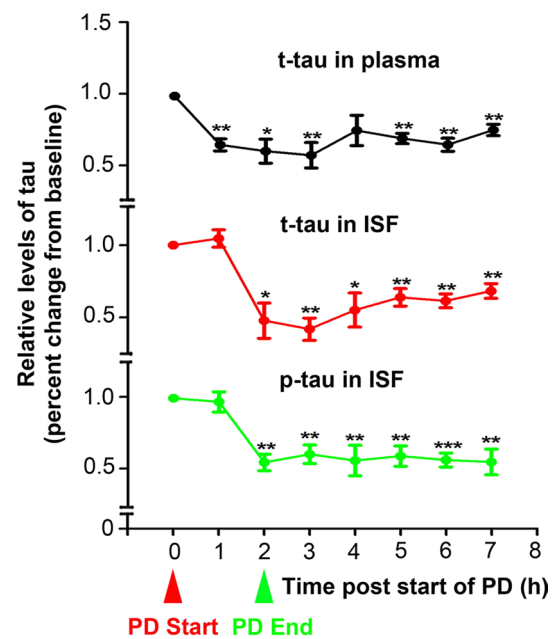


Fig. 2 Dynamic changes in tau levels in brain ISF and blood from pR5 mice treated with peritoneal dialysis. To explore whether lowering tau levels in the blood could affect central tau levels, peritoneal dialysis was performed in 3-month-old male pR5 mice, and dynamic changes in tau levels in brain ISF and blood were measured. PD peritoneal dialysis. $n=5$ each timepoint. Error bar, SEM. * $p < 0.05$, ** $p < 0.01$, and *** $p < 0.001$, paired t test

together. We injected ^{131}I -tau into the cisterna magna of one parabiotic mouse (ipsilateral parabionts) and observed the dynamic distribution of tau in the brain, kidney, blood, and liver of both ipsilateral and contralateral parabiotic mice. Singular Wt mice were used as the control. As shown in Fig. 1c, at 15 min after injection, radioactivity was mainly detectable in the blood of contralateral mice. During the following 4 h, radioactivity levels in the blood, kidney, and liver increased remarkably over time (Fig. 1c). These results indicate that tau effluxed from the brain into the blood and was then transferred to contralateral mice via circulation, finally being cleared in the peripheral tissues and organs of contralateral mice. In ipsilateral parabionts, radioactivity in the brain, blood, and kidney declined faster than in singular mice (Fig. 1d, Supplemental Fig. 1e), suggesting that the addition of another set of peripheral tissues and organs accelerated tau efflux from brain and its clearance in the periphery.

Parabiosis alleviates tau pathologies in the brain

To investigate the effects of physiological tau clearance in the periphery on tau pathologies in the brain, we utilized isochronic parabiosis between pR5 mice and their sex-matched Wt littermates. After 3 months of parabiosis,

blood t-tau levels in the parabiotic pR5 mice were significantly lower than those in control pR5 mice and were comparable to those in parabiotic Wt mice (Supplemental Fig. 2b). In addition, t-tau levels in the kidney were significantly reduced, and t-tau in the liver also tended to decrease (Supplemental Fig. 2c, d). These findings suggest that the parabiosis models were successfully established and that the additional viscera from parabiotic Wt mice took up tau proteins from pR5 mice.

Next, we compared phosphorylated tau levels between parabiotic pR5 mice and control pR5 mice 3 months after parabiosis. Immunohistochemical assays showed that phospho-Tau(pS396)-positive staining in the hippocampus and neocortex of pa(3–6 mo) pR5 mice decreased by approximately 25% (Fig. 3a). Similarly, AT100-positive staining was also reduced in the amygdala after parabiosis (Fig. 3a). Using Western blot assays, we measured the levels of tau phosphorylation at additional epitopes and found that the levels of tau phosphorylation at the Ser404 (pS404), Thr231 (pT231), Ser199 (pS199), and Thr181 (pT181) epitopes were also reduced in pa(3–6 mo) pR5 mice, whereas total tau (tau5) showed a tendency to decline, but the decrease was not statistically significant (Fig. 3b). One possible explanation is that the majority of total tau was normal tau protein bound to microtubules and thus would not be influenced by physiological peripheral clearance. Next, we examined p-tau levels in different solubility fractions and found that the levels of both pT231-tau and pT181-tau were reduced in the TBS fraction (soluble) as well as in the SDS fraction (insoluble) in parabiotic pR5 mice relative to controls (Fig. 3c), with a total reduction (including both soluble and insoluble tau species) of 23.44% for pT231 and 21.03% for pT181.

We investigated mechanisms underlying the reduction of tau phosphorylation other than direct tau clearance after parabiosis. GSK-3 β is a critical enzyme that induces tau phosphorylation. We found that the brain pS9-GSK3 β :GSK3 β ratio was elevated in pa(3–6 mo) pR5 mice, suggesting that the activity of GSK3 β was reduced after parabiosis (Fig. 3d).

Parabiosis alleviates neurodegeneration and neuroinflammation

Compared with control pR5 mice, pa(3–6 mo) pR5 mice exhibited an increased proportion of staining for Map-2 in the hippocampal CA1 region (Fig. 4a, c) and a decreased proportion of activated caspase-3 in the hippocampus CA3 region (Fig. 4b, c). Then, using Western blot assays, we found that the immunoreactivities of synapse-related proteins, including SYP, SNAP-25, and VAMP-1, and proteins associated with neural regeneration, including NSE and DCX, were significantly elevated after parabiosis

(Fig. 4e–g). These findings suggest that parabiosis alleviated neurodegeneration in the brain of pa(3–6 mo) pR5 mice.

We measured pro-inflammatory factors in both the brain and blood (Fig. 4d, Supplemental Fig. 3). The results showed that both IFN- γ and TNF- α , but not IL-1 β or IL-6, were significantly reduced in the brains of pa(3–6 mo) pR5 mice compared with control pR5 mice, which were comparable to Wt mice (Fig. 4d). These findings suggest that parabiosis protected against neuroinflammation in the brain.

Finally, we measured the LTP of the hippocampal CA1 region. As shown in Fig. 4h, HFS induced reliable LTP in Wt mice, but the LTP was significantly weaker in pR5 mice than in Wt mice, indicating that the plasticity of the examined synapses is impaired in the brains of pR5 mice. However, no significant difference in LTP was observed between parabiotic and control pR5 mice. This may be because the limited reduction of phosphorylated tau (<25%) was insufficient to improve LTP.

Discussion

In the present study, we showed that tau in the brain can efflux into the blood and is cleared in the periphery; acute enhancement of peripheral tau clearance facilitates tau efflux from the brain; and chronic enhancement of peripheral tau clearance alleviates pathological tau accumulation, neurodegeneration, and neuroinflammation in the brain. Our findings provide the first evidence that physiological tau clearance occurs in the periphery, which makes a significant contribution to pathological tau clearance from the brain.

The prerequisite for physiological tau clearance in the periphery is that tau in the brain can efflux into blood. We found that synthesized human tau was detectable in the blood within minutes after injection into the cisterna magna of Wt mice, and these findings are consistent with the previous studies [35, 45] and provide compelling evidence that tau in the brain can egress to the periphery. However, the efflux mechanism is not yet well understood. To date, specific tau transporters across the blood–brain barrier have not been identified. Instead, tau is thought to egress into blood via the glymphatic system or CSF absorption from the arachnoid villi and blood–CSF barrier or from the lymphatic system [17, 27, 37, 42]. These efflux pathways need to be verified, and other pathways need to be identified in the future. Where does brain-derived tau go after efflux out of the brain? We found that tau can be cleared in the periphery, particularly in the blood, kidney, and liver, under physiological conditions in mice and humans. These are also the main tissues and organs for clearance of A β , a major causative molecule of AD [39, 41]. In the circulation, tau might be phagocytized by monocytes, which are suggested to have tau clearance capacity in the brain [13], as well as by other immunocytes

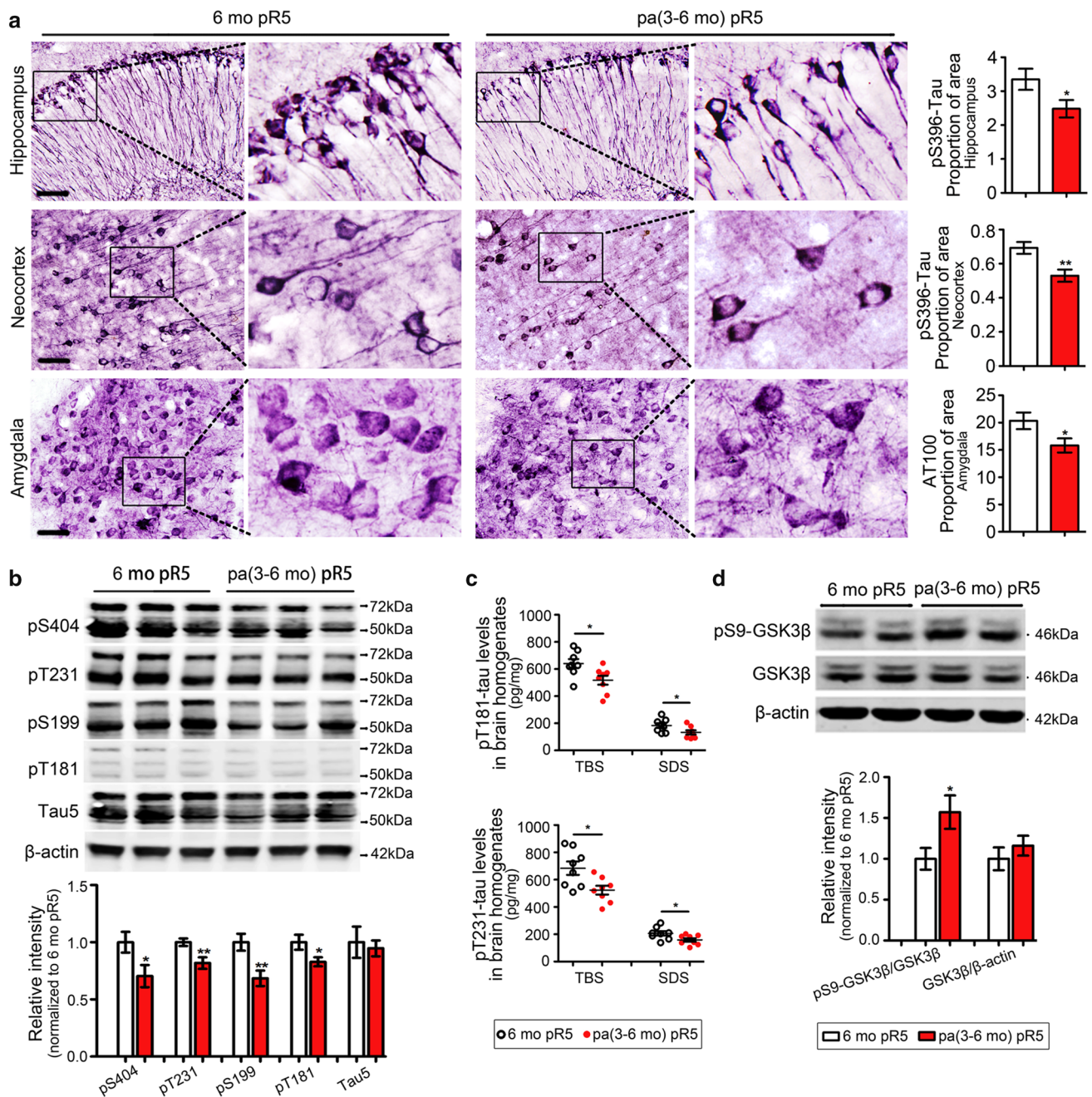


Fig. 3 Parabiosis reduces abnormally phosphorylated tau in the pR5 mouse brain. **a** Representative images of pS396-tau and PHF-tau (AT100) immunohistochemical staining in the hippocampus, neocortex and amygdala in 6 mo pR5 and pa(3–6 mo) pR5 mice; the proportion of area stained positive for pS396 in the hippocampus and neocortex and that for AT100 in the amygdala were reduced in pa(3–6 mo) pR5 mice relative to control pR5 mice. Scale bars 50 μ m. **b** Western blot assays of total tau (tau5) and phosphorylated tau at mul-

tipule sites, including Ser404, Thr231, Ser199, and Thr181, in brain homogenates from 6 mo pR5 and pa(3–6 mo) pR5 mice. **c** Quantitative comparison of pT231-tau and pT181-tau levels, measured via ELISA, in TBS and 2% SDS fractions of brain extracts between 6 mo pR5 and pa(3–6 mo) pR5 mice. **d** Western blot assays of pS9-GSK3 β and total GSK3 β levels in the two pR5 groups. $n=8$ per group; error bar SEM. * $p<0.05$, and ** $p<0.01$, Student's t test

[31]. Like A β , tau might also be bound and transported by albumin, erythrocytes, or other blood components [39]. In the kidney and liver, tau may be degraded and/or excreted with urine or bile. These speculations need to be verified in

future studies. It has been proposed that there is an equilibrium between intracellular tau and extracellular tau [4]. In our study, peritoneal dialysis removed blood tau and further induced a reduction in tau levels in ISF, suggesting that there

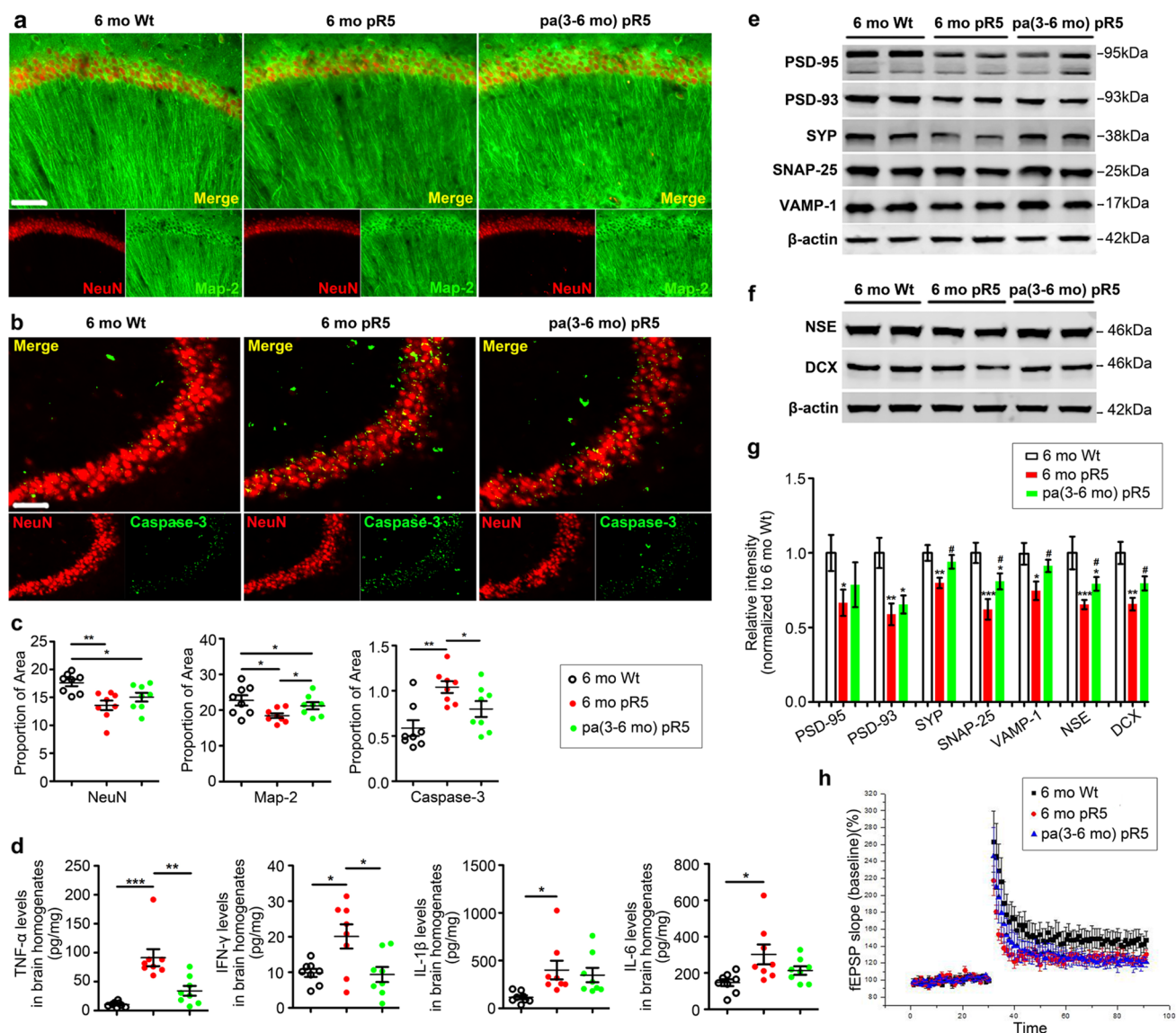


Fig. 4 Parabiosis rescues neurodegeneration and neuroinflammation. **a** Representative images of neurons and dendrites in the CA1 region of the hippocampus stained with anti-NeuN and anti-Map-2 immunofluorescent antibodies in pa(3–6 mo) pR5, control pR5 and wild-type (Wt) mice. Scale bars 50 μ m. **b** Representative images of neuronal apoptosis in the CA3 region of the hippocampus stained with activated caspase-3 immunofluorescent antibody in pa(3–6 mo) pR5, 6 mo pR5 and 6 mo Wt mice. Scale bars 50 μ m. **c** Quantitative comparison of the proportion of area stained positive for NeuN, Map-2 and caspase-3 among pa(3–6 mo) pR5 mice, 6 mo pR5 mice and 6 mo Wt mice. **d** Quantitative comparison of pro-inflammatory factor levels in brain homogenates among pa(3–6 mo) pR5, 6 mo pR5 and 6 mo Wt

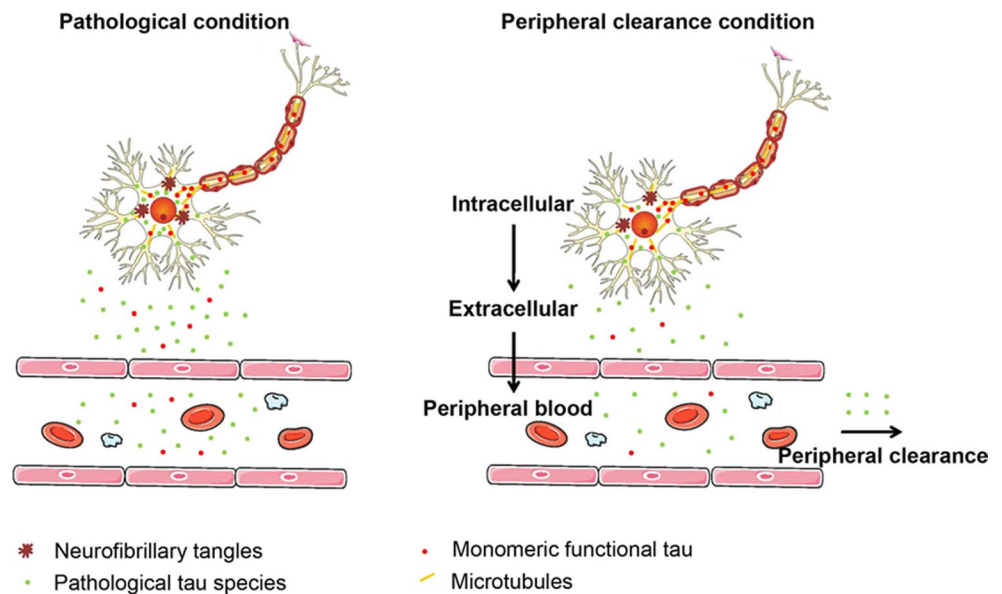
mice. **e** Western blot assays of synapse-associated proteins, including PSD-95, PSD-93, SYP, SNAP-25, and VAMP-1, in brain homogenates from the three groups of mice. **f** Western blot assays of neurogenesis biomarkers, including NSE and DCX, in brain homogenates from the three groups of mice. **g** Quantitative comparison of the densities of the PSD-95, PSD-93, SYP, SNAP-25, VAMP-1, NSE, and DCX bands among pa(3–6 mo) pR5, 6 mo pR5 and 6 mo Wt mice. **h** Hippocampal CA1 long-term potentiation (LTP) in pa(3–6 mo) pR5, 6 mo pR5 and 6 mo Wt mice. **a–g** $n=8$ per group; **h** $n=6$ per group; error bar, SEM. *Represents comparison with 6 mo Wt mice, and # represents comparison with 6 mo pR5 mice; * $p<0.05$, ** $p<0.01$, *** $p<0.001$, and # $p<0.05$, one-way ANOVA

is also an equilibrium between brain extracellular tau and blood tau levels. Taken together, our findings suggest that there is an equilibrium among intracellular and extracellular tau pools in the brain and tau pools in peripheral blood; depletion of peripheral blood tau shifts the equilibrium between the brain and blood tau pools, thereby leading to

removal of extracellular tau in ISF and then of intracellular tau, thus inducing clearance of pathological tau in the brain (Fig. 5).

Our findings reveal the occurrence of physiological tau clearance in the periphery. How competent this process is in removal of brain tau remains unknown. We used a parabiosis

Fig. 5 Schematic mechanism of peripheral clearance. There is an equilibrium among intracellular and extracellular tau pools in the brain and the peripheral blood; depletion of peripheral blood tau shifts the equilibrium between the brain and blood tau pools, thereby leading to removal of extracellular tau in ISF and then of intracellular tau, thus inducing clearance of pathological tau in the brain



model to calculate the contribution of a singular peripheral system to brain tau clearance. On the basis of our results, the brain pathological tau burden in a transgenic mouse is defined as 100%, and the reduction by an additional peripheral system is 23.44% as reflected by ELISA analysis of pT231. Thus, the total pathological tau in the brain of a transgenic mouse without peripheral clearance should be $100 + 23.44\%$. Using the following equation: clearance rate of a singular periphery = reduction of brain pathological tau in a parabiotic transgenic mouse/total pathological tau in the brain of a transgenic mouse without an additional peripheral system, we calculate that a singular peripheral system can remove approximately 19% of pathological tau from the brain in a pR5 mouse. The amount of hyperphosphorylated tau cleared from the brain by the peripheral system is much less than that of A β , which was found to be approximately 40% in our previous study [41]. This might be because A β is mainly accumulated extracellularly, while hyperphosphorylated tau mainly accumulates intracellularly, and thus, removal through the peripheral clearance pathway is harder.

It is worth noting that in addition to direct removal of tau, other mechanisms may also contribute to the reduction of tau pathologies in the brain after parabiosis. GSK3 β is an extensively studied tau phosphorylation enzyme, and its activation leads to tau phosphorylation. In our study, the activity of GSK3 β was reduced after parabiosis. There might be a feedback loop between GSK3 β activation and tau phosphorylation: reduced phosphorylated tau leads to less GSK3 β activation, and in turn, reduced GSK3 β activation may further lead to decreased tau phosphorylation [38]. Inflammation is suggested to exacerbate tau pathologies [1, 19, 26]. In our present study, parabiosis decreases inflammatory factors, such as TNF- α and IFN- γ , in the

brain of parabiotic pR5 mice, which can regulate the activity of GSK3 β and thus may influence tau phosphorylation [14, 30]. How competent does the reduced inflammation contribute to tau reduction after parabiosis? In pR5 mouse brains, we observed rare activated microglia, which are abundant in AD mouse models, suggesting that pR5 mice have lower neuroinflammation levels than AD mice. The levels of TNF- α and IFN- γ in the blood were not significantly different between pR5 and Wt mice, implying that parabiosis between pR5 and Wt mice may not be sufficiently potent to directly reduce inflammatory cytokines in the blood and then in the brain of parabiotic pR5 mice. Thus, the reduced brain tau levels after parabiosis might be mainly due to tau clearance, although alleviated neuroinflammation might also play a role in this process. The above findings suggest that parabiosis reduces tau pathologies in the brain through multiple pathways.

Our findings provide insight into the pathogenesis of tauopathies. In our previous study, we put forward the systemic view of AD that systemic abnormalities not only develop secondary to brain dysfunction, but also affect AD progression and proposed that systemic factors might interact with brain-related factors to modify the AD development process [39]. Here, we found that tau could also be cleared in the periphery. It is intriguing to speculate that compromised peripheral function might impede tau clearance from the brain and thereby contribute to disease pathogenesis. A recent study reported that peripheral administration of tau aggregates can trigger brain tau pathology in tau transgenic mice [6]. Whether the peripheral pool of tau is associated with or causally linked to tauopathies, and whether and how the brain and periphery interact with each other to affect the progression of tauopathies are unknown. Elucidation of

these questions could significantly improve our understanding of the pathogenesis of tauopathies.

Tau-targeting therapies are important approaches for tauopathies. Most previous efforts to inhibit tau phosphorylation kinases, tau aggregation, or stabilize microtubules have been discontinued during or before clinical trials due to toxicity or lack of efficacy [2, 7, 32]. Currently, tau clearance using immunotherapy has become more attractive, and some of these treatments have exhibited promising therapeutic potential in preclinical testing and have progressed to clinical trials [7, 23]. Our study provides evidence that enhancement of tau clearance in the periphery is a potent method to reduce tau pathologies in the brain, suggesting that peripheral tau clearance is a promising therapeutic strategy for tauopathies.

Our present study has implications for understanding tau-related pathogenesis and for development of treatments for other neurodegenerative diseases, such as Parkinson's disease (PD), Huntington's disease (HD), amyotrophic lateral sclerosis (ALS), and non-tau frontotemporal lobar degeneration (FTLD). The pathogenic proteins associated with these diseases, such as α -synuclein, mutant huntingtin protein (mHtt), and TDP-43, and circulating constituents, such as exosomes and immune cells, which are likely derived from the brain, are elevated in patient plasma [9, 11, 24, 36, 40]. Therefore, clearance of brain-derived pathological proteins in the periphery seems to be a universal physiological process, and enhancing peripheral clearance may be a potential approach to treating these neurodegenerative diseases.

In conclusion, our study reveals the physiological contribution of the periphery to clearance of pathological brain tau and provides proof-of-concept evidence that therapies for tauopathies could focus on enhancing peripheral tau clearance. Our study also implies that reduction of inflammatory factors via peripheral approaches may also help alleviating tau pathologies in the brain. In addition, our findings highlight the importance of understanding the pathogenesis of neurodegenerative diseases and developing therapeutics for these diseases through a systemic approach.

Acknowledgements This study was supported by the National Natural Science Foundation of China (NSFC) through Grants 81625007, 91749206, and 81600949. The authors would like to thank the following for aid in radiolabelling of ^{131}I -tau: Professor Ding-De Huang from Department of Nuclear Medicine, Southwest Hospital of Third Military Medical University, and Professor Zhi-Ping Peng from Department of Radiological Medicine, College of Basic Medical, Chongqing Medical University. The authors would also like to thank professor Shi-Fei Tong from The Third Affiliated Hospital of Chongqing Medical University for collecting blood samples from patients.

Compliance with ethical standards

Conflict of interest The authors have declared that no conflict of interest exists.

References

- Barron M, Gartlon J, Dawson LA, Atkinson PJ, Pardon MC (2017) A state of delirium: deciphering the effect of inflammation on tau pathology in Alzheimer's disease. *Exp Gerontol* 94:103–107. <https://doi.org/10.1016/j.exger.2016.12.006>
- Brunden KR, Trojanowski JQ, Lee VM (2009) Advances in tau-focused drug discovery for Alzheimer's disease and related tauopathies. *Nat Rev Drug Discov* 8:783–793. <https://doi.org/10.1038/nrd2959>
- Bu XL, Xiang Y, Jin WS, Wang J, Shen LL, Huang ZL, Zhang K, Liu YH, Zeng F, Liu JH et al (2017) Blood-derived amyloid-beta protein induces Alzheimer's disease pathologies. *Mol Psychiatry*. <https://doi.org/10.1038/mp.2017.204>
- Castillo-Carranza DL, Sengupta U, Guerrero-Munoz MJ, Lasagna-Reeves CA, Gerson JE, Singh G, Estes DM, Barrett AD, Dineley KT, Jackson GR et al (2014) Passive immunization with Tau oligomer monoclonal antibody reverses tauopathy phenotypes without affecting hyperphosphorylated neurofibrillary tangles. *J Neurosci* 34:4260–4272. <https://doi.org/10.1523/JNEUROSCI.3192-13.2014>
- Chiotis K, Saint-Aubert L, Rodriguez-Vieitez E, Leuzy A, Almkvist O, Savitcheva I, Jonasson M, Lubberink M, Wall A, Antoni G et al (2017) Longitudinal changes of tau PET imaging in relation to hypometabolism in prodromal and Alzheimer's disease dementia. *Mol Psychiatry*. <https://doi.org/10.1038/mp.2017.108>
- Clavaguera F, Hench J, Lavenir I, Schweighauser G, Frank S, Goedert M, Tolnay M (2014) Peripheral administration of tau aggregates triggers intracerebral tauopathy in transgenic mice. *Acta Neuropathol* 127:299–301. <https://doi.org/10.1007/s00401-013-1231-5>
- Congdon EE, Sigurdsson EM (2018) Tau-targeting therapies for Alzheimer disease. *Nat Rev Neurol*. <https://doi.org/10.1038/s41582-018-0013-z>
- Dage JL, Wennberg AMV, Airey DC, Hagen CE, Knopman DS, Machulda MM, Roberts RO, Jack CR Jr, Petersen RC, Mielke MM (2016) Levels of tau protein in plasma are associated with neurodegeneration and cognitive function in a population-based elderly cohort. *Alzheimer's Dement J Alzheimer's Assoc* 12:1226–1234. <https://doi.org/10.1016/j.jalz.2016.06.001>
- De Marco G, Lupino E, Calvo A, Moglia C, Buccinna B, Grifoni S, Ramondetti C, Lomartire A, Rinaudo MT, Piccinini M et al (2011) Cytoplasmic accumulation of TDP-43 in circulating lymphomonocytes of ALS patients with and without TARDBP mutations. *Acta Neuropathol* 121:611–622. <https://doi.org/10.1007/s00401-010-0786-7>
- Deters N, Ittner LM, Gotz J (2008) Divergent phosphorylation pattern of tau in P301L tau transgenic mice. *Eur J Neurosci* 28:137–147. <https://doi.org/10.1111/j.1460-9568.2008.06318.x>
- Foulds P, McAuley E, Gibbons L, Davidson Y, Pickering-Brown SM, Neary D, Snowden JS, Allsop D, Mann DM (2008) TDP-43 protein in plasma may index TDP-43 brain pathology in Alzheimer's disease and frontotemporal lobar degeneration. *Acta Neuropathol* 116:141–146. <https://doi.org/10.1007/s00401-008-0389-8>
- Guo T, Noble W, Hanger DP (2017) Roles of tau protein in health and disease. *Acta Neuropathol* 133:665–704. <https://doi.org/10.1007/s00401-017-1707-9>
- Gyoneva S, Kim D, Katsumoto A, Kokiko-Cochran ON, Lamb BT, Ransohoff RM (2015) Ccr2 deletion dissociates cavity size and tau pathology after mild traumatic brain injury. *J Neuroinflamm* 12:228. <https://doi.org/10.1186/s12974-015-0443-0>
- Hu X, Paik PK, Chen J, Yarilina A, Kockeritz L, Lu TT, Woodgett JR, Ivashkiv LB (2006) IFN-gamma suppresses IL-10

- production and synergizes with TLR2 by regulating GSK3 and CREB/AP-1 proteins. *Immunity* 24:563–574. <https://doi.org/10.1016/j.immuni.2006.02.014>
15. Iba M, Guo JL, McBride JD, Zhang B, Trojanowski JQ, Lee VM (2013) Synthetic tau fibrils mediate transmission of neurofibrillary tangles in a transgenic mouse model of Alzheimer's-like tauopathy. *J Neurosci* 33:1024–1037. <https://doi.org/10.1523/JNEUROSCI.2642-12.2013>
 16. Iba M, McBride JD, Guo JL, Zhang B, Trojanowski JQ, Lee VM (2015) Tau pathology spread in PS19 tau transgenic mice following locus coeruleus (LC) injections of synthetic tau fibrils is determined by the LC's afferent and efferent connections. *Acta Neuropathol* 130:349–362. <https://doi.org/10.1007/s00401-015-1458-4>
 17. Iliff JJ, Chen MJ, Plog BA, Zeppenfeld DM, Soltero M, Yang L, Singh I, Deane R, Nedergaard M (2014) Impairment of glymphatic pathway function promotes tau pathology after traumatic brain injury. *J Neurosci* 34:16180–16193. <https://doi.org/10.1523/JNEUROSCI.3020-14.2014>
 18. Iqbal K, Liu F, Gong CX (2016) Tau and neurodegenerative disease: the story so far. *Nat Rev Neurol* 12:15–27. <https://doi.org/10.1038/nrneurol.2015.225>
 19. Janelsins MC, Mastrangelo MA, Park KM, Sudol KL, Narrow WC, Oddo S, LaFerla FM, Callahan LM, Federoff HJ, Bowers WJ (2008) Chronic neuron-specific tumor necrosis factor- α expression enhances the local inflammatory environment ultimately leading to neuronal death in 3xTg-AD mice. *Am J Pathol* 173:1768–1782. <https://doi.org/10.2353/ajpath.2008.080528>
 20. Jiao SS, Shen LL, Zhu C, Bu XL, Liu YH, Liu CH, Yao XQ, Zhang LL, Zhou HD, Walker DG et al (2016) Brain-derived neurotrophic factor protects against tau-related neurodegeneration of Alzheimer's disease. *Transl Psychiatry* 6:e907. <https://doi.org/10.1038/tp.2016.186>
 21. Jin WS, Shen LL, Bu XL, Zhang WW, Chen SH, Huang ZL, Xiong JX, Gao CY, Dong Z, He YN et al (2017) Peritoneal dialysis reduces amyloid-beta plasma levels in humans and attenuates Alzheimer-associated phenotypes in an APP/PS1 mouse model. *Acta Neuropathol* 134:207–220. <https://doi.org/10.1007/s00401-017-1721-y>
 22. Josephs KA, Murray ME, Tosakulwong N, Whitwell JL, Knopman DS, Machulda MM, Weigand SD, Boeve BF, Kantarci K, Petrucelli L et al (2017) Tau aggregation influences cognition and hippocampal atrophy in the absence of beta-amyloid: a clinico-imaging-pathological study of primary age-related tauopathy (PART). *Acta Neuropathol* 133:705–715. <https://doi.org/10.1007/s00401-017-1681-2>
 23. Khanna MR, Kovalevich J, Lee VM, Trojanowski JQ, Brunden KR (2016) Therapeutic strategies for the treatment of tauopathies: hopes and challenges. *Alzheimer's Dement J Alzheimer's Assoc* 12:1051–1065. <https://doi.org/10.1016/j.jalz.2016.06.006>
 24. Le W, Dong J, Li S, Korczyn AD (2017) Can biomarkers help the early diagnosis of Parkinson's disease? *Neurosci Bull* 33:535–542. <https://doi.org/10.1007/s12264-017-0174-6>
 25. Lewis J, Dickson DW (2016) Propagation of tau pathology: hypotheses, discoveries, and yet unresolved questions from experimental and human brain studies. *Acta Neuropathol* 131:27–48. <https://doi.org/10.1007/s00401-015-1507-z>
 26. Li Y, Liu L, Barger SW, Griffin WS (2003) Interleukin-1 mediates pathological effects of microglia on tau phosphorylation and on synaptophysin synthesis in cortical neurons through a p38-MAPK pathway. *J Neurosci* 23:1605–1611
 27. Louveau A, Smirnov I, Keyes TJ, Eccles JD, Rouhani SJ, Peske JD, Derecki NC, Castle D, Mandell JW, Lee KS et al (2015) Structural and functional features of central nervous system lymphatic vessels. *Nature* 523:337–341. <https://doi.org/10.1038/nature14432>
 28. Mandelkow EM, Mandelkow E (2012) Biochemistry and cell biology of tau protein in neurofibrillary degeneration. *Cold Spring Harbor Perspect Med* 2:a006247. <https://doi.org/10.1101/cshperspect.a006247>
 29. Orr ME, Sullivan AC, Frost B (2017) A brief overview of tauopathy: causes, consequences, and therapeutic strategies. *Trends Pharmacol Sci* 38:637–648. <https://doi.org/10.1016/j.tips.2017.03.011>
 30. Park SH, Park-Min KH, Chen J, Hu X, Ivashkiv LB (2011) Tumor necrosis factor induces GSK3 kinase-mediated cross-tolerance to endotoxin in macrophages. *Nat Immunol* 12:607–615. <https://doi.org/10.1038/ni.2043>
 31. Pascual G, Wadia JS, Zhu X, Keogh E, Kukrer B, van Ameijde J, Inganas H, Siregar B, Perdok G, Diefenbach O et al (2017) Immunological memory to hyperphosphorylated tau in asymptomatic individuals. *Acta Neuropathol* 133:767–783. <https://doi.org/10.1007/s00401-017-1705-y>
 32. Polanco JC, Li C, Bodea LG, Martinez-Marmol R, Meunier FA, Gotz J (2017) Amyloid-beta and tau complexity—towards improved biomarkers and targeted therapies. *Nat Rev Neurol*. <https://doi.org/10.1038/nrneurol.2017.162>
 33. Santa-Maria I, Varghese M, Ksiezak-Reding H, Dzhun A, Wang J, Pasinetti GM (2012) Paired helical filaments from Alzheimer disease brain induce intracellular accumulation of Tau protein in aggregates. *J Biol Chem* 287:20522–20533. <https://doi.org/10.1074/jbc.M111.323279>
 34. Shen LL, Manucat-Tan NB, Gao SH, Li WW, Zeng F, Zhu C, Wang J, Bu XL, Liu YH, Gao CY et al (2018) The ProNGF/p75NTR pathway induces tau pathology and is a therapeutic target for FTLT-tau. *Mol Psychiatry*. <https://doi.org/10.1038/s41380-018-0071-z>
 35. Shi M, Kovac A, Korff A, Cook TJ, Ghingina C, Bullock KM, Yang L, Stewart T, Zheng D, Aro P et al (2016) CNS tau efflux via exosomes is likely increased in Parkinson's disease but not in Alzheimer's disease. *Alzheimer's Dement J Alzheimer's Assoc* 12:1125–1131. <https://doi.org/10.1016/j.jalz.2016.04.003>
 36. Shi M, Liu C, Cook TJ, Bullock KM, Zhao Y, Ghingina C, Li Y, Aro P, Dator R, He C et al (2014) Plasma exosomal alpha-synuclein is likely CNS-derived and increased in Parkinson's disease. *Acta Neuropathol* 128:639–650. <https://doi.org/10.1007/s00401-014-1314-y>
 37. Tarasoff-Conway JM, Carare RO, Osorio RS, Glodzik L, Butler T, Fieremans E, Axel L, Rusinek H, Nicholson C, Zlokovic BV et al (2015) Clearance systems in the brain—implications for Alzheimer disease. *Nat Rev Neurol* 11:457–470. <https://doi.org/10.1038/nrneurol.2015.119>
 38. Vossel KA, Xu JC, Fomenko V, Miyamoto T, Suberbielle E, Knox JA, Ho K, Kim DH, Yu GQ, Mucke L (2015) Tau reduction prevents Abeta-induced axonal transport deficits by blocking activation of GSK3beta. *J Cell Biol* 209:419–433. <https://doi.org/10.1083/jcb.201407065>
 39. Wang J, Gu BJ, Masters CL, Wang YJ (2017) A systemic view of Alzheimer disease—insights from amyloid-beta metabolism beyond the brain. *Nat Rev Neurol* 13:612–623. <https://doi.org/10.1038/nrneurol.2017.111>
 40. Weiss A, Trager U, Wild EJ, Grueninger S, Farmer R, Landles C, Scahill RI, Lahiri N, Haider S, Macdonald D et al (2012) Mutant huntingtin fragmentation in immune cells tracks Huntington's disease progression. *J Clin Invest* 122:3731–3736. <https://doi.org/10.1172/JCI64565>
 41. Xiang Y, Bu XL, Liu YH, Zhu C, Shen LL, Jiao SS, Zhu XY, Giunta B, Tan J, Song WH et al (2015) Physiological amyloid-beta clearance in the periphery and its therapeutic potential for Alzheimer's disease. *Acta Neuropathol* 130:487–499. <https://doi.org/10.1007/s00401-015-1477-1>

42. Xin SH, Tan L, Cao X, Yu JT, Tan L (2018) Clearance of amyloid beta and tau in Alzheimer's disease: from mechanisms to therapy. *Neurotox Res*. <https://doi.org/10.1007/s12640-018-9895-1>
43. Yamada K, Holth JK, Liao F, Stewart FR, Mahan TE, Jiang H, Cirrito JR, Patel TK, Hochgrafe K, Mandelkow EM et al (2014) Neuronal activity regulates extracellular tau in vivo. *J Exp Med* 211:387–393. <https://doi.org/10.1084/jem.20131685>
44. Yanamandra K, Kfoury N, Jiang H, Mahan Thomas E, Ma S, Maloney Susan E, Wozniak David F, Diamond Marc I, Holtzman David M (2013) Anti-tau antibodies that block tau aggregate seeding in vitro markedly decrease pathology and improve cognition in vivo. *Neuron* 80:402–414. <https://doi.org/10.1016/j.neuron.2013.07.046>
45. Yanamandra K, Patel TK, Jiang H, Schindler S, Ulrich JD, Boxer AL, Miller BL, Kerwin DR, Gallardo G, Stewart F et al (2017) Anti-tau antibody administration increases plasma tau in transgenic mice and patients with tauopathy. *Sci Transl Med*. <https://doi.org/10.1126/scitranslmed.aal2029>
46. Yao XQ, Jiao SS, Saadipour K, Zeng F, Wang QH, Zhu C, Shen LL, Zeng GH, Liang CR, Wang J et al (2015) p75NTR ectodomain is a physiological neuroprotective molecule against amyloid-beta toxicity in the brain of Alzheimer's disease. *Mol Psychiatry* 20:1301–1310. <https://doi.org/10.1038/mp.2015.49>
47. Zou H, Wen C, Peng Z, Shao Y, Hu L, Li S, Li C, Zhou HH (2018) P4HB and PDIA3 are associated with tumor progression and therapeutic outcome of diffuse gliomas. *Oncol Rep* 39:501–510. <https://doi.org/10.3892/or.2017.6134>